Published in final edited form as:

Mol Psychiatry. 2021 December ; 26(12): 7509–7521. doi:10.1038/s41380-021-01187-x.

Cerebellin-2 Regulates a Serotonergic Dorsal Raphe Circuit that Controls Compulsive Behaviors

Erica Seigneur, Ph.D.[1,#,*], **Jie Wang, Ph.D.**[1], **Jinye Dai, Ph.D.**[1], **Jai Polepalli, Ph.D.**[1,#], **Thomas C. Südhof, M.D.**[1,*]

[1]Dept. of Molecular Cellular Physiology and Howard Hughes Medical Institute, Stanford University School of Medicine, 265 Campus Dr., Stanford, CA 94305 USA

Abstract

Cerebellin-1 (Cbln1) and cerebellin-2 (Cbln2) are secreted glycoproteins that are expressed in distinct subsets of neurons throughout the brain. Cbln1 and Cbln2 simultaneously bind to presynaptic neurexins and postsynaptic GluD1 and GluD2, thereby forming *trans*-synaptic adhesion complexes. Genetic associations link cerebellins, neurexins and GluD's to neuropsychiatric disorders involving compulsive behaviors, such as Tourette syndrome, attention-deficit hyperactivity disorder (ADHD), and obsessive-compulsive disorder (OCD). Extensive evidence implicates dysfunction of serotonergic signaling in these neuropsychiatric disorders. Here, we report that constitutive Cbln2 KO mice, but not Cbln1 KO mice, display robust compulsive behaviors, including stereotypic pattern running, marble burying, explosive jumping, and excessive nest building, and exhibit decreased brain serotonin levels. Strikingly, treatment of Cbln2 KO mice with the serotonin precursor 5-hydroxytryptophan or the serotonin reuptake-inhibitor fluoxetine alleviated compulsive behaviors. Conditional deletion of Cbln2 both from dorsal raphe neurons and from presynaptic neurons synapsing onto dorsal raphe neurons reproduced the compulsive behaviors of Cbln2 KO mice. Finally, injection of recombinant Cbln2 protein into the dorsal raphe of Cbln2 KO mice largely reversed their compulsive behaviors. Taken together, our results show that Cbln2 controls compulsive behaviors by regulating serotonergic circuits in the dorsal raphe.

INTRODUCTION

Neurodevelopmental disorders of compulsivity (Tourette syndrome and obsessive-compulsive disorder [OCD]) and impulsivity (attention-deficit hyperactivity disorder [ADHD] and impulsive aggression) are characterized by behavioral disinhibition (the inability to resist expressing inappropriate behaviors [1,2]). These disorders are thought

[*]Addresses for correspondence (seign3eur@stanford.edu or tcs1@stanford.edu.

[#]Present addresses: E.S., Dept. of Psychiatry and Behavioral Sciences, Stanford University School of Medicine, 1201 Welch Rd., Stanford, CA 94305 USA; J.P., Healthy Longevity Translational Research Program, Yong Loo Lin School of Medicine, National University of Singapore

CONFLICT OF INTEREST

The authors declare no conflict of interest

to involve a common molecular pathway [2,3,4,5]. Similar to schizophrenia, these disorders contain a large genetic component [6,7], and are associated with a dysfunction of the serotonergic system [8,9,10].

Cbln1 and Cbln2 belong to a family of secreted proteins (Cbln1–4) that mediate assembly of *trans*-synaptic cell-adhesion complexes. Cbln1 and Cbln2 simultaneously bind to presynaptic neurexins and postsynaptic GluD1 and GluD2 (a.k.a. GluRδ1 and GluRδ2), thereby connecting presynaptic terminals to postsynaptic specializations [11,12,13,14,15] (reviewed in 16,17). Neurexins are expressed by three genes (*NRXN1-NRXN3* in humans) [18,19,20,21] that are associated with multiple neuropsychiatric disorders, including Tourette syndrome, schizophrenia, and autism [5,6,22]. Mutations in the GluD1 gene (gene symbol *GRID1*) have also been found in schizophrenia and bipolar disorder [23,24,25,26], while a recent genome-wide association study linked the *GRID2* gene to OCD [27]. Together, these data suggest that disruption of the Nrxn1/2/3-Cbln2-GluD1/2 complex may contribute to the pathogenesis of neuropsychiatric disorders characterized by behavioral disinhibition.

Although the neural mechanisms underlying neuropsychiatric disorders are poorly understood, dysfunction of the serotonergic system of the dorsal raphe (DR) likely plays a central role [2,28,29,30,31,32,33,34,35,36,37]. Recently, we used conditionally mutant Cbln2-mVenus reporter mice to identify Cbln2-expressing neurons in the DR and in brain nuclei that regulate DR neurons [38]. This led to the hypothesis that Cbln2 is involved in the regulation of the DR serotonergic system, and that therefore loss of Cbln2 could lead to dysfunction of this system and to increased behavioral disinhibition.

Here, we report that constitutive Cbln2 KO mice are hyperactive, hyperaggressive, and engage in compulsive behaviors, including explosive jumping and excessive nestbuilding. We link these behaviors to a dysfunction of the serotoninergic system by showing that in Cbln2 KO mice, explosive jumping and excessive nest building are ameliorated by treatment with the serotonin precursor 5-hydroxytryptophan or the serotonin reuptake inhibitor fluoxetine. Moreover, we document that the Cbln2 KO significantly decreased the serotonin concentration in multiple brain regions. Strikingly, simultaneous genetic deletion of Cbln2 in DR neurons and in neurons projecting to the DR induced explosive jumping in mice, while injection of recombinant Cbln2 protein into the DR of Cbln2 KO mice ameliorated explosive jumping. Taken together, our results reveal an unexpected control of compulsive behaviors by a Cbln2-dependent mechanism in the DR that regulates synapses formed on serotonergic neurons. Moreover, our results suggest that Cbln2 KO mice could serve as a translational model to study disorders of behavioral disinhibition, such as Tourette syndrome, OCD, and ADHD.

RESULTS

Cbln2 KO mice exhibit disinhibited, repetitive behaviors, whereas Cbln1 KO mice display decreased anxiety.

We tested constitutive Cbln1 and Cbln2 KO mice [15] in behavioral assays that monitor spontaneous activity, anxiety, and various forms of behavioral disinhibition. On a force-

plate actometer used to measure open-field activity, both Cbln1 and Cbln2 KO mice were hyperactive and traveled significantly larger distances than control littermates (P=0.005; Fig. 1a). Cbln1, but not Cbln2, KO mice additionally spent more time in the center of the field than control mice (adj. P=0.035, Dunnett's *post hoc;* Fig. 1b), consistent with previous findings that whole brain and cerebellum-only Cbln1 KO mice exhibit decreased anxiety in the open field test [14]. Cbln2 KO mice, conversely, engaged in compulsive circling/running and produced significantly more rotations around the center of the open field than control mice, whereas Cbln1 KO mice exhibited significantly fewer rotations (P=0.008; Fig. 1c). Strikingly, Cbln2 KO mice often displayed an explosive jumping behavior that was absent from Cbln1 KO mice (see below and Supplementary Video 1). Lastly, both Cbln1 KO and Cbln2 KO mice exhibited significantly larger stereotypy scores, calculated by measuring a mouse's activity level in a confined space (P=0.032; Fig. 1d).

We next tested anxiety-like behaviors using an elevated plus maze. Again, Cbln1 but not Cbln2 KO mice showed decreased anxiety. Cbln1 KO mice spent approximately twice as much time than control and Cbln2 KO mice in the open arms (P=0.019; Fig. 1e), spent less time in the closed arms (P=0.030; Supplementary Fig. S1a), and made significantly more entries into the open arms (P=0.042; Fig. 1f). The Cbln2 KO mice, conversely, traveled more than twice the distance on the elevated plus-maze (P=0.015; Fig. 1g) at approximately twice the velocity (P=0.013; Fig. 1h) than control and Cbln1 KO mice. Both KO mice also made more entries into the closed arms than control mice (P=0.039; Supplementary Fig. S1a). Combined, these results suggest that both Cbln1 and Cbln2 KO mice are hyperactive on the elevated plus maze, but that Cbln1 KO mice spend more time in the open arms than control or Cbln2 KO mice, whereas Cbln2 KO mice are engaged in compulsive pattern running, moving back and forth between the two closed arms. This assessment was confirmed by reviewing video recordings of the trials after data analysis was complete.

Cbln2 KO mice exhibit increased, and Cbln1 KO mice decreased, aggressive behavior.

Using the resident/intruder test to assess aggressive behavior, we found that Cbln1 KO mice initiated significantly fewer attacks compared to control mice, whereas Cbln2 KO mice initiated significantly more attacks (P=0.026; Fig. 1i). The same trend was seen in the latency to initiate the first attack, with Cbln1 KO mice showing a longer, and Cbln2 KO mice a shorter, latency to attack compared to control mice, although these trends did not reach statistical significance (P=0.086; Fig. 1i). We also observed that male Cbln2 KO mice tended to engage in violent aggressive behaviors towards littermates when group-housed, resulting in injury or death if not separated. These same mice sometimes displayed a "hard to handle" phenotype – struggling, jumping, and attempting to bite in response to human handling [2,39].

Cbln2, but not Cbln1, KO mice engage in compulsive marble burying, explosive jumping, and excessive nest building.

We next examined compulsive behaviors using marble burying and nest building tests [2,32,33,34]. In the marble burying test, which measures compulsive digging, Cbln2 KO mice buried significantly more marbles than control or Cbln1 KO mice (P=0.032; Fig. 1j). Moreover, we observed that when placed in an open field arena, Cbln2 KO mice exhibited

compulsive, novelty-induced explosive jumping (Fig. 1k; Supplementary Video 1). Because this behavior was most pronounced in mice aged 4–6 weeks [31], we quantified explosive jumping in 1-month-old mice. Explosive jumping was rarely detected in control and Cbln1 KO mice, but regularly observed in Cbln2 KO mice (P=0.0002) (Fig. 1k).

Nest building is a normal important mouse behavior that is often used to assess general health and basic cognitive function (Fig. 1l) [40]. We provided single-housed male mice with nest building material (a square cotton “nestlet”) and scored the nest quality 24 hours later, but observed no differences between Cbln1 KO, Cbln2 KO, and control mice (Fig. 1m). However, when we provided the mice with a cardboard tube for burrowing in addition to nestlets, we found that some mice used the tube as additional nesting material, eventually creating massive nests. We quantified this ‘excessive’ nest building by assigning each nest a score from 0–3 based on the percentage of tube a mouse had incorporated into the nest (Fig. 1n). Control and Cbln1 KO mice incorporated ~10–50% of the tube material into a nest, whereas Cbln2 KO mice incorporated 80–100% (P<0.0001; Fig. 1o).

Cbln1 or Cbln2 deletions do not induce depression-like behaviors.

We next tested the Cbln1 and Clbn2 KO mice for anhedonia and learned helplessness using the sucrose preference and forced swim tests [41]. In the sucrose preference test, we measured how much water vs. a 2% sucrose solution, offered as a free choice, a mouse consumed. No difference between control, Cbln1 KO, and Cbln2 KO mice was detected, suggesting that the Cbln1 or Cbln2 KO mice do not suffer from anhedonia (Supplementary Fig. S1b). Similarly, the forced swim test revealed no differences between control, Cbln1 KO, and Cbln2 KO mice in the time spent immobile or the latency to immobility (Supplementary Fig. S1c). Combined, these results show that genetic deletion of Cbln1 or Cbln2 has no effect on depression-like behaviors in mice.

Genetic deletion of Cbln2, but not of Cbln1, decreases the forebrain serotonin concentration.

Based on our behavioral results, we hypothesized that the Cbln2 KO might affect the brain’s serotoninergic or dopaminergic systems that are linked to compulsive behaviors [28,42,43]. To test this hypothesis, we measured the serotonin and dopamine concentrations in the prefrontal cortex (PFC) and striatum of littermate control, constitutive Cbln1 KO, and Cbln2 KO mice by ELISA. Compared to control mice, the serotonin concentration was unchanged in the PFC and striatum of Cbln1 KO mice, but significantly decreased in the PFC (~40%; P=0.005) and striatum (~50%; P=0.0015) of Cbln2 KO mice (Fig. 2a). Conversely, the dopamine concentration was unchanged in the PFC, but significantly increased in the striatum of both Cbln1 and Cbln2 KO mice compared to control mice (P=0.0004; Fig. 2b), with a ~70% increase in Cbln1 KO mice (adj. P<0.0002, Dunnett’s *post hoc*) and a ~30% increase in Cbln2 KO mice (adj. P=0.055, Dunnett’s *post hoc*) (Fig. 2b). Previous studies showed that hyperactivity and motor stereotypy are caused by increased dopaminergic activity in the forebrain [28,43]. The presence of these behaviors in both Cbln1 and Cbln2 KO mice (Fig. 1) is therefore consistent with, and supported by, the increased dopamine concentration in the striatum.

To further characterize the serotonergic system in Cbln2 KO mice, we measured with ELISAs in a new cohort of Cbln2 KO and littermate control mice the concentrations of 5-HT and the 5-HT metabolite 5-hydroxyindoleacetic acid (5-HIAA) in multiple brain regions. These experiments confirmed that the concentration of 5-HT was significantly decreased in the PFC (~50%; P=0.0044), striatum (~30%; P=0.0069), and hippocampus (~40%; P=0.0366), but was unchanged in the amygdala and dorsal raphe (DR) of Cbln2 KO mice (Fig. 2c). 5-HIAA was unchanged in most brain regions except for the striatum (~30% decrease; P=0.0255) (Fig. 2c). Thus, the Cbln2 KO impairs the serotoninergic system in multiple brain regions.

Increasing the serotonin levels in Cbln2 KO mice reverses explosive jumping and excessive nest building phenotypes.

Previous studies have linked explosive jumping and excessive nest building to decreased serotonin signaling and demonstrated that these behaviors are rescued by administration of the serotonin precursor, 5-hydroxytryptophan, or of serotonin reuptake inhibitors [29,31,37]. We therefore tested if explosive jumping and excessive nest building could also be rescued in Cbln2 KO mice by increasing the brain's serotonin levels. We measured baseline jumping in an open field in 1-month-old mice, injected the mice 7 days later intraperitoneally with saline, 10 mg/kg 5-hydroxytryptophan, or 10 mg/kg fluoxetine, and placed the mice back into the arena after a 30 min recovery period to measure post-treatment jumping (Fig. 2d). As above (Fig. 1k), at baseline Cbln2 KO mice engaged in massively increased explosive jumping compared to control mice (P<0.0001; Fig. 2e) 5-hydroxytryptophan or fluoxetine greatly reduced explosive jumping in Cbln2 KO mice (P<0.0001 for both), whereas saline had no effect (Fig. 2e).

To determine if excessive nest building by Cbln2 KO mice is also due to decreased serotonin signaling, we again first measured baseline nest building for 4 days. Every day, single-housed mice were offered 9 grams of cotton nesting material, nests were removed after 24 hours and the amount of unused nesting material was weighed; the mice were then given 9 grams of new cotton nesting material. After 4 days of baseline measurements, mice were then given a 2% sucrose control solution or a 2% sucrose solution containing fluoxetine (50 mg/kg), and nest building was measured again for 4 days. Similar to our earlier observations (Fig. 1o), Cbln2 KO mice engaged in excessive nest building, using significantly more cotton than control littermates at baseline and in the 2% sucrose control group (P=0.0018; Fig. 2f). Fluoxetine significantly decreased nest building behavior in both control and Cbln2 KO mice (P<0.0001; Fig. 2f), such that after fluoxetine treatment, control and Cbln2 KO mice were no longer statistically significantly different. In these experiments, we used a slightly different protocol for measuring nest building than in the experiments described above (Fig. 1l–1o) to enable a faster experimental throughput. Combined, these results support the hypotheses that deletion of Cbln2 impairs the serotonergic system in the brain, and that the resulting decrease in serotonin concentration induces compulsive behaviors in Cbln2 KO mice.

Cbln2 is expressed in a subset of serotonergic DR neurons.

To determine how Cbln2 affects the serotonin system, we analyzed Cbln2 expression in serotonergic neurons by immunohistochemistry. Neurons in the DR and median raphe (MR) provide most serotoninergic inputs to the forebrain [44,45]. The DR is divided into dorsal (DRD), ventral (DRV), intrafascicular (DRI), and posterodorsal (PDR) subnuclei [45]. Using Cbln2-mVenus reporter mice [38], we observed $Cbln2^+$ neurons throughout the DR and MR, with the highest density observed in the DRV and DRI (Fig. 3a, 3b). Since serotonergic neurons comprise only 25–50% of neurons in the DR and 20–30% of neurons in the MR [44], we stained Cbln2-mVenus brain sections for tryptophan hydroxylase 2 (TPH2), the rate-limiting enzyme for serotonin synthesis. In the DRV and DRI, 53% and 59% of $TPH2^+$ neurons, respectively, co-expressed Cbln2, while 94% and 92% of $Cbln2^+$ neurons were $TPH2^+$ (Fig. 3b; Supplementary Table S1). In the PDR, 54% of $TPH2^+$ neurons co-expressed Cbln2, and 69% of $Cbln2^+$ neurons were $TPH2^+$, although both cell types exhibited a much lower density than in the DRV and DRI. Little co-expression was observed in other raphe nuclei (Fig. 3c; Supplementary Table S1). Together, these results show that Cbln2 is expressed in >50% of serotoninergic neurons in the DRV and DRI, and that nearly all (>90%) of the Cbln2-expressing neurons in these subnuclei are serotonergic.

Conditional deletion of Cbln2 from serotonergic neurons alone does not reproduce the constitutive Cbln2 KO phenotype.

The robust expression of Cbln2 in serotonergic neurons of the DR raises the possibility that Cbln2 expression in serotonergic neurons is essential for serotonergic signaling. To test this possibility, we crossed conditional Cbln2 KO mice with SERT-Cre mice that selectively express Cre-recombinase in serotonergic neurons [46]. However, deletion of Cbln2 from serotonergic neurons failed to induce explosive jumping, even though in this experiment Cbln2 is deleted not only from serotonergic neurons, but also from some non-serotonergic neurons that express SERT transiently during development [47](Supplementary Fig. S2). This result indicates that the loss of Cbln2 from serotonergic output synapses does not cause the observed phenotype.

Cbln2 is expressed in a subset of neurons that project to the DR.

Since the loss of Cbln2 from serotonergic neurons alone did not explain the phenotype, we asked whether it was possible that Cbln2 was involved in the tight regulation of serotonin neurons by input synapses derived from non-serotonergic nuclei of the brain [30,45,48,49,50,51,52]. In order to test if Cbln2 is expressed in neurons that regulate the activity of serotonergic neurons in the DR, we injected the retrograde tracer cholera toxin B (CTB) into the DR of Cbln2-mVenus mice and quantified the number of $CTB^+/Cbln2^+$ double-positive neurons throughout the brain. Similar to previous studies [45,48], neurons with abundant projections to the DR were observed in the PFC, hypothalamus, lateral habenula, and the interpeduncular nucleus (Fig. 3d–3k; Supplementary Fig. S3). CTB^+ neurons were also observed in regions where Cbln2 was not expressed or where no CTB/Cbln2 co-expression was observed and were therefore not included in this analysis.

In the PFC, we observed abundant CTB^+ neurons in the agranular insula (AI), orbital frontal (ORB), anterior cingulate (ACC), prelimbic (PrL), and limbic (IL) areas (Fig. 3d–

3h). Although Cbln2 is highly expressed in these areas [38], the number of $CTB^+/Cbln2^+$ double-positive neurons varied. The greatest overlap was found in the AI (Fig. 3e) and the lateral (ORBl) and ventral (ORBv) subregions of the ORB (Fig. 3f) (Supplementary Table S2). Cbln2 was also expressed in CTB^+ neurons of the ACC (Fig. 3g), PrL (Fig. 4h), IL, and medial ORB, but at lower levels (Supplementary Table S2). $CTB^+/Cbln2^+$ double-labeled neurons were found at lower density in the motor cortex, claustrum, and the retrosplenial cortex (Supplementary Table S2). Outside of the cortex, large numbers of $CTB^+/Cbln2^+$ neurons were observed in the lateral habenula (LHb) (Fig. 3i, 3j; Supplementary Table S2), which sends direct excitatory projections to the DR [45,53]. Moreover, neurons in the interpeduncular nucleus (IPN) that form inhibitory projections to the DR [45] were densely labeled by CTB. Since neurons in the medial habenula (MHb) primarily project to the IPN [53,54] and express high levels of Cbln2 [55], Cbln2 may exert indirect regulatory control over DR neurons via the MHb-IPN pathway. In addition to this indirect inhibitory input, a small number of CTB^+ neurons that co-expressed Cbln2 were also observed in the MHb, suggesting the MHb also provides direct excitatory input to the DR (Fig. 3k; Supplementary Table S2). Interestingly, these CTB^+ neurons were only found in the superior portion of the ventrolateral MHb and in region "X," which is thought to contain a mixture of MHb and LHb neurons [56], and therefore may function as a unique regulator of DR activity. In addition, $CTB^+/Cbln2^+$ double-labeled neurons were observed in the preoptic and periventricular nuclei of the hypothalamus, although at lower density than in the cortex or habenula (Supplementary Table S2). Combined, these results show that Cbln2 is highly expressed in important input hubs to the DR and may therefore play a role in regulating the top-down control of serotonin neurons.

Cbln2 KO alters the synaptic proteome of the DR without decreasing the density of synapses or neurons.

To determine if loss of Cbln2 affects the number of serotonergic neurons, we quantified the density of serotonergic and of total neurons in the DR using immunohistochemistry for TPH2 and NeuN in Cbln2 KO mice, but found no change (Supplementary Fig. S4). Moreover, the TPH2 immunofluorescence signal intensity of neurons was also unchanged.

Next, we quantified the number of excitatory synapses in the DR by immunohistochemistry for the vesicular glutamate transporters vGluT1 and vGluT2. Again, we detected no change. The size or density of $vGluT1^+$ or $vGluT2^+$ puncta on $TPH2^+$ neurons in the DRV, which represent inputs arising largely from the PFC and LHb, respectively [51], were indistinguishable between control and Cbln2 KO mice (Fig. 4a–d).

In a previous study, we found that the Cbln2 KO alters the synaptic proteome in multiple forebrain regions [15]. This finding motivated us to test whether the Cbln2 KO changes the expression of select synaptic proteins and of TPH2 in the DR (Fig. 4e–f). Consistent with the immunohistochemistry data, the levels of TPH2 were unchanged in Cbln2 KO mice. Moreover, the levels of the serotonin-1A (5-HT1A) receptor, which functions as an inhibitory autoreceptor of serotonergic neurons [57], were also not altered. However, the levels of GluA2, an AMPA-receptor subunit, were increased ~35% in Cbln2 KO mice (P=0.0101), and the levels GluN1 and GluN2A, two NMDA-receptor subunits, were

increased ~40% (P=0.0494) and ~60% (P=0.0464), respectively. Conversely, the levels of another NMDA-receptor subunit, GluN2B, were decreased ~30%, but this change was not statistically significant (P=0.0879; Fig. 4e–f).

Cbln2 KO decreases the density of vGluT3$^+$ serotonergic synapses in the anterior cingulate cortex.

Does the Cbln2 KO alter the development of serotonergic axons and target synapses? To address this question we first quantified SERT$^+$ axons and SERT$^+$ puncta in multiple brain regions. We detected no changes in the density of SERT$^+$ axons and the density and size of SERT$^+$ puncta in Cbln2 KO mice in the anterior cingulate cortex (Fig. 4g–k), striatum, CA1 region of the hippocampus, or basolateral amygdala (Supplementary Fig. S5). We then examined the effect of Cbln2 deletion on excitatory synapses arising from serotonergic DR neurons, using immunohistochemistry for the vesicular glutamate transporter vGluT3, which exhibits limited expression in the brain overall, but is expressed in most serotonergic neurons of the DR and MR [58,59,60]. vGluT3 enhances vesicular packaging of serotonin and is targeted to a subset of serotoninergic nerve terminals [33,61,62], suggesting that presynaptic vGluT3-containing varicosities represent a subtype of serotoninergic synapses. Synapses containing SERT (a marker for serotonergic neurons) but lacking vGluT3 (SERT$^+$/vGluT3$^-$) and synapses containing both SERT and vGluT3 (SERT$^+$/vGluT3$^+$), therefore, represent two functional classes of serotoninergic synapses. We quantified the density and size of SERT$^+$/vGluT3$^-$ and SERT$^+$/vGluT3$^+$ puncta in the mPFC, focusing on the ACC (Fig. 4j–k). Compared to control littermates, the relative density of SERT$^+$/vGluT3$^-$ puncta was increased in Cbln2 KO mice by ~20% (P=0.0015), whereas the relative density of SERT$^+$/vGluT3$^+$ puncta was decreased by ~40% (P=0.0005; Fig. 4j–k). We also observed a small (~12%) but significant decrease in the size of SERT$^+$/vGluT3$^+$ synapses in Cbln2 KO mice compared to control mice (P=0.0117), but detected no difference in the size of SERT$^+$/vGluT3$^-$ synapses between the two groups (Fig. 4j–k).

Together, these data suggest that the Cbln2 deletion causes a shift in the molecular properties of serotonergic synapses in the mPFC.

Conditional deletion of Cbln2 both from the DR and from neurons projecting to the DR is required to induce explosive jumping.

We showed earlier that the Cbln2 KO phenotype is not due to a loss of Cbln2 from serotonergic DR neurons (Supplementary Fig. S2). However, Cbln2 functions as a secreted *trans*-synaptic organizer that could be supplied to DR synapses by the presynaptic inputs onto the serotonergic neurons even if Cbln2 expression is deleted from these neurons. To test this possibility, we used a viral strategy that selectively deletes Cbln2 in (1) neurons in the DR, (2) neurons projecting to the DR, or (3) both types of neurons. We then examined the mice for explosive jumping. To selectively delete Cbln2 from DR neurons, we stereotactically injected adeno-associated viruses (AAVs) expressing active (Cre) or inactive mutant Cre-recombinase (ΔCre; control) under control of the synapsin-1 promoter into the DR of conditional Cbln2 KO mice at P18–P21. To selectively delete Cbln2 from neurons projecting to the DR, we injected retrograde AAVs (rAAVs) expressing Cre under control of the synapsin-1 promoter [63]. Finally, to delete Cbln2 both from DR neurons *and* from

neurons projecting to the DR, we injected both AAV-syn-Cre and rAAV-Syn-Cre into the DR (Fig. 5a, 5b; Supplementary Fig. S6). Two weeks later, we placed the mice in an open field arena and measured explosive jumping.

Selective deletion of Cbln2 in DR neurons alone using a viral strategy did not induce explosive jumping, consistent with our genetic results (Figs. 5c, S2). Selective deletion of Cbln2 in neurons projecting to the DR also did not replicate the explosive jumping phenotype (Fig. 5c). However, deletion of Cbln2 from both the DR neurons and the neurons projecting to the DR produced explosive jumping ($P<0.0001$; Fig. 5c). Thus, loss of Cbln2 from the serotonergic circuit of the DR underlies explosive spontaneous jumping activity as a proxy for compulsive behaviors.

Infusion of recombinant Cbln2 into the DR decreases explosive jumping in Cbln2 KO mice.

The observation that either presynaptic or postsynaptic expression of Cbln2 in the DR maintains its function is surprising, raising the question whether Cbln2 is truly required for the normal function of a serotonergic circuit in the DR that controls compulsive behaviors. An alternative hypothesis might be that Cbln2 also performs a broader action outside of the DR in the neurons synapsing onto serotonergic DR neurons. To address this key question, we were inspired by previous studies showing that in Cbln1 KO mice, application of recombinant Cbln1 protein onto Purkinje cells rescues the motor deficits [64,65]. This amazing finding suggested that the effect of the genetic Cbln1 deletion is rapidly reversible by simple addition of extrinsic Cbln1 protein. Thus, we asked whether a similar rescue might be produced by application of recombinant Cbln2 into the DR of constitutive Cbln2 KO mice.

We stereotactically injected either vehicle (control) or recombinant His-tagged Cbln2 (4 μg/μl) into the DR of 1 month-old constitutive Cbln2 KO mice, and used antibodies against the His-tag and TPH2 to visualize the distribution of Cbln2 protein among serotonergic neurons after 2–14 days (Fig. 5d; Supplementary Fig. S7). In Cbln2 treated mice, Cbln2-His immunoreactivity was observed throughout the DR at 2- and 4-days post-injection, with a punctate pattern on the dendrites and cell bodies of $TPH2^+$ neurons. The Cbln2-His signal was significantly diminished by day 7, and undetectable by day 14.

To determine if introducing Cbln2 protein into the DR rescues the explosive jumping phenotype of constitutive Cbln2 KO mice, we measured baseline jumping of Cbln2 KO mice in an open field arena, stereotactically injected vehicle or Cbln2-His (4 μg/μl) into their DR 7 days later, and examined explosive jumping again at 4 days post-injection. Strikingly, explosive jumping was significantly decreased in Cbln2-treated mice compared to baseline (adj. $P=0.013$, Sidak's *post hoc*), whereas explosive jumping was not significantly changed in the vehicle-treated mice (Fig. 5e). This finding, combined with the results described above, indicates that Cbln2 directly regulates a serotonergic circuit in the DR, and that dysfunction of this regulation causes behavioral disinhibition, including explosive jumping.

DISCUSSION

Recent genetic studies have associated the genes encoding Cbln2 and its binding partners, neurexins and GluD1/2, with Tourette syndrome and other disorders of behavioral disinhibition, such as ADHD and OCD [5,6,7,22,23,25,26,27]. Abundant evidence suggests that decreased brain serotonin signaling contributes to the pathogenesis of these disorders [2,29,31,32,36,37]. Here, we report that Cbln2 regulates the circuits of the DR that control serotonergic signaling throughout the brain, thus connecting the human genetics to the phenotype of disorders of behavioral disinhibition. Loss of Cbln2 induced compulsive behaviors in mice, such that the mice became hyperactive, engaged in stereotypic movements, exhibited continuous explosive jumping in a novel environment, and built excessive nests. This phenotype was associated with a robust decrease in serotonin concentrations in multiple forebrain regions. Remarkably, the phenotype was only induced when Cbln2 was deleted from both DR neurons and Cbln2-expressing neurons that form synapses onto DR neurons. In constitutive Cbln2 KO mice that exhibit compulsive jumping behavior, injection of Cbln2 protein into the DR alone partly rescued the phenotype. Importantly, Cbln1 was not functionally redundant with Cbln2, as deletion of Cbln1 had no effect on the serotonergic system and did not produce disinhibition behaviors.

Based on its similarity to the human condition and established animal models, we propose the Cbln2 KO mouse as a translational model to study disorders of behavioral disinhibition. The validity of animal models of human mental disorders is assessed using three criteria: (1) face validity: how similar is the animal phenotype to the human disorder, (2) construct validity: how well do the behavioral assays used measure the behavioral features of the human disorder, and (3) predictive validity: to what extent therapeutics used to treat symptoms in the human disorder alleviate the symptoms in the animal model [41]. We showed that Cbln2 KO mice engaged in a number of behaviors that (1) are homologous to the human disorder, (2) have been observed in mouse models of Tourette syndrome, OCD, and ADHD, and (3) have been linked to dysfunction of the serotonergic system and are treated by increasing brain serotonin. Specifically, we showed that Cbln2 KO mice were hyperactive, aggressive, and displayed motor stereotypy, all of which are characteristic of human patients and of mouse models of Tourette syndrome [66,67], OCD [32,34,36,37], and ADHD [28]. These symptoms are commonly treated with serotonin reuptake inhibitors and/or psychostimulants, both of which increase the concentration of serotonin in brain [28,43], which also alleviated the disinhibition symptoms of Cbln2 KO mice.

Cbln2 KO mice also engaged in compulsive marble burying and excessive nest building, which are well-established assays for stereotypic and compulsive goal-directed behaviors observed in Tourette syndrome and OCD. Both behaviors have been used to validate mouse models of OCD [2,34,36,37]. Moreover, both behaviors are partly rescued by increasing the brain serotonin concentration using treatments with 5-hydroxytryptophan or serotonin reuptake inhibitors [2,32,34,36,37]. We similarly found that treatment with the serotonin reuptake inhibitor fluoxetine significantly reduced excessive nest building in Cbln2 KO mice.

Lastly, Cbln2 KO mice engaged in compulsive pattern running and explosive jumping, which model compulsive and repetitive motor actions characteristic of Tourette syndrome and OCD [34,36,37]. Interestingly, mice lacking the neuropeptide PACAP also engaged in compulsive and explosive jumping, which similar to the Cbln2 KO mice was significantly reduced following IP injection of 5-hydroxytryptophan or fluoxetine [29,31]. These findings, along with the rescue of the excessive nest building phenotype by fluoxetine, supports the hypothesis that the decrease in brain serotonin induced by the Cbln2 KO results in disinhibited behaviors characteristic of Tourette syndrome and OCD. Taken together, our data thus show that the Cbln2 KO mouse has face, construct, and predictive validity as a translational model for Tourette syndrome, OCD, and ADHD.

Summary.

Viewed together, our data show that a trans-synaptic adhesion molecule, Cbln2, functions as a fundamental regulator of synapses on serotonergic neurons in the DR. Loss of Cbln2 causes behavioral disinhibition, manifesting as compulsive spontaneous jumping, excessive nest building, increased marble burying, and stereotypic movements. These results suggest a pathway by which mutations in genes related to the Cbln2-based trans-synaptic adhesion complex, namely neurexins, cerebellins, and GluDs, might predispose to neuropsychiatric disorders with a strong compulsive component, and establish the Cbln2 KO mouse as a model system for neuropsychiatric disinhibition symptoms.

MATERIALS AND METHODS

Mouse handling and husbandry.

All experiments were performed with male and female young adult, C57/Bl6/SV129 hybrid mice. All animal procedures conformed to National Institutes of Health's *Guidelines for the Care and Use of Laboratory Animals* and were approved by the Stanford University Administrative Panel on Laboratory Animal Care. Sample sizes were chosen based prior studies from our lab [15,38,55].

Immunohistochemistry.

Experiments were carried out as described previously [38] and in the Extended Materials and Methods. 3-week-old Cbln2-mVenus mice were used for retrograde tracing and co-labeling experiments, and at least two mice and four sections per mouse were used for analysis. 1-month-old male Cbln2 KO and control littermates were used for axon and synapse quantification experiments in Fig. 4. For each synaptic marker, data were collected from 3 mice/genotype, 3 sections/mouse. The density of $vGluT1^+$ and $vGluT2^+$ synapses was first normalized to the area of TPH2-labeled tissue and then to the density observed in the controls. The density of $SERT^+$ and $vGluT3^+$ synapses was first normalized to the area of SERT-labeled axons and then to the density observed in the controls. $SERT^+$ axon density was quantified using the DEFiNE plugin for ImageJ/Fiji [68] and was first normalized to the area of the region of interest and then to the density observed in the controls. 1-month-old male and female Cbln2 KO mice were used for the Cbln2-His labeling experiments. Two mice and four sections per mouse were collected for each time point in the Cbln2 treated group and for the vehicle treated group. Images were

collected using a Nikon A1R confocal with a 60X objective and analyzed using NIS-Elements Advanced Research software (Nikon Instruments) or ImageJ/Fiji (NIH). The following antibodies were used in this study: monoclonal mouse anti-6xHis (1:200; 75-169 NeuroMab; RRID: AB_10673446), polyclonal rabbit anti-Cre-Recombinase (1:250, 257 003 Synaptic Systems; RRID: AB_2619968), polyclonal chicken anti-GFP (1:1000; GFP-1020 Aves Labs; RRID: AB_10000240), polyclonal guinea pig anti-NeuN (1:500; ABN90P Millipore; RRID: AB_2341095), polyclonal rabbit anti-TPH2 (1:1000; NB100-74555 Novus; RRID: AB_2202792), monoclonal mouse anti-SERT (1:200; NBP1-78989 Novus; RRID: AB_11006862), polyclonal guinea pig anti-vGluT1 (1:500; AB5905 Millipore; RRID: AB_2301751), polyclonal guinea pig anti-vGluT2 (1:500; AB2251 Millipore; RRID: AB_1587626), and polyclonal rabbit anti-vGluT3 (1:500; 135 203 Synaptic Systems; RRID: AB_887886).

Retrograde tracing.

Adult (P30–P40) Cbln2-mVenus mice were anesthetized with tribromoethanol (125–200 mg/kg), and 1ul (0.5 μl at each depth) of 0.25% cholera toxin-B (CTB) conjugated to Alexa 647 (ThermoFisher Scientific) was stereotactically injected into the dorsal raphe at a flow rate of 0.15 μl/min (coordinates from Bregma: ML: 0 mm, AP: −4.5 mm, DV: −2.8 mm and −3.5 mm). Mice were sacrificed after 3 weeks and sections were analyzed by fluorescence microscopy following the protocol described in the Extended Materials and Methods.

Measurement of serotonin and dopamine by ELISA.

Concentrations of serotonin, 5-HIAA, and dopamine were measured in tissue samples using Serotonin High Sensitive ELISA kit (Eagle Biosciences), 5-HIAA ELISA kit (Novus Biologicals), and Dopamine ELISA kit (Eagle Biosciences), respectively, according to the manufacturer's instructions. Monoamine concentrations were first normalized to the concentration of total protein in the sample and then to the values in the control samples. Samples were collected from 6 mice/genotype, and 3 samples/genotype were tested in two separate assays. In the first set of experiments, tissues were taken from ~1-month-old littermate control, Cbln1 KO, and Cbln2 KO mice (Fig. 2a–b); in the second set of experiments, tissues were taken from ~1-month-old littermate control and Cbln2 KO mice (Fig. 2c).

Immunoblotting.

Experiments were carried out as described previously [15] and in the Extended Materials and Methods. Samples were prepared from microdissections of the dorsal raphe taken from ~1-month-old Cbln2 KO mice and control littermates. Intensity values for each protein of interest were first normalized to β-actin and then to the values in the control samples. Samples were collected from 6 mice/group. The following antibodies were used in this study: monoclonal mouse anti-β-actin (1:5000; A1978 Sigma-Aldrich; RRID: AB_476692), polyclonal rabbit anti-GluA1 (1:500; PC246 Millipore; RRID: AB_564636), monoclonal mouse anti-GluA2 (1:1000; MAB397 Millipore; RRID: AB_2113875), polyclonal rabbit anti-GluA4 (1:1000; AB1508 Millipore; RRID: AB_90711), monoclonal mouse anti-GluN1 (1:500; 114011 Synaptic Systems; RRID: AB_887750), monoclonal mouse anti-GluN2A (1:500; 75-288 Neuromab; RRID: AB_2315842), monoclonal mouse anti-GluN2B

(1:500; 75-097 Neuromab; RRID: AB_10673405), polyclonal rabbit anti-HTR1A (1:1000; PA5-99483 Thermo Fisher Scientific; RRID: AB_2818416), and polyclonal rabbit anti-TPH2 (1:1000; NB100-74555 Novus; RRID: AB_2202792).

Stereotaxic injections.

Viral injections were carried out on Cbln2$^{Flox/Flox}$ mice aged P18–P21. Mice were anesthetized with tribromoethanol (125–200 mg/kg), and viral solution was injected (0.5 μl at each depth) into the DR at a flow rate of 0.15 μl/min (coordinates from Bregma: ML: 0 mm, AP: −4.5 mm, DV: −3.0 mm and −3.4 mm). AAVs packaged into AAV-DJ capsids and using the synapsin promoter to drive expression of GFP and either inactive Cre-recombinase (AAV-DJ-Syn-ΔCre-GFP) or active Cre-recombinase (AAV-DJ-Syn-Cre-GFP) and retrograde AAV packaged into the rAAV-retro2 capsid and using the synapsin promoter to drive expression of active Cre-recombinase (rAAV-retro-Syn-Cre-GFP) were purchased from the Neuroscience Gene Vector and Virus Core at Stanford University. Explosive jumping behavior was assessed 2 weeks after injection. Injections of recombinant Cbln2 protein (tagged and purified with 6xHis) were carried out on Cbln2 KO mice aged P35–P40. Either vehicle (control) or a 4 μg/μl solution of recombinant Cbln2-His was injected (0.5 μl at each depth) into the DR at a flow rate of 0.15 μl/min, using the same coordinates as above. Explosive jumping behavior was assessed 4 days after injection.

Mouse behavior.

To generate Cbln1 KO or Cbln2 KO mice, homozygous Cbln1$^{flox/flox}$ or Cbln2$^{flox/flox}$ mice were crossed with transgenic mice expressing Cre-recombinase under control of the nestin promoter (Jackson Labs), as described previously [15]. All behavior experiments were done using male littermate control, Cbln1 KO, and Cbln2 KO mice aged 2–4 months, excepted where noted (see also Extended Materials and Methods). For the conditional knockout experiments, male and female Cbln2$^{Flox/Flox}$ mice were used. Where applicable, mice were randomly assigned to treatment groups. All experiments were carried out between 7am–7pm. Mice were moved from the holding facility to the testing room at least 1h before testing began. All behavior assays were conducted and analyzed by researchers blind to genotype. Detailed descriptions of behavior assays are found in the Extended Materials and Methods.

Statistics.

All statistical analysis was done using GraphPad Prism 6. Graphs depict mean ± S.E.M. Neuron, axon, and puncta quantifications were analyzed with Student's t-test and significant differences are reported as p-values. ELISA measurements and behavior assays comparing control, Cbln1 KO, and Cbln2 KO mice were analyzed by one-way Kruskal-Wallis analysis of variance (ANOVA) for group differences and significant differences are reported as p-values. Differences between control and individual KO groups were then determined using Dunnett's post hoc test, correcting for multiple comparisons, and are reported as adjusted p-values. ELISA measurements, immunoblots, and behavior comparing control and Cbln2 KO mice were analyzed by Student's t-test and significant differences are reported as p-values. For the rescue experiments with 5-hydroxytryptophan or fluoxetine, data were analyzed by two-way ANOVA for group comparisons and significant differences are reported as

p-values. Within group treatment comparisons were then determined using Tukey's post hoc test, correcting for multiple comparisons, and significant differences are reported as adjusted p-values.

Supplementary Material

Refer to Web version on PubMed Central for supplementary material.

ACKNOWLEDGEMENTS

This study was supported by a grant from the NIMH (MH052804 to T.C.S.).

REFERENCES

1. Iacono WG, Malone SM, McGue M. Behavioral disinhibition and the development of early-onset addiction: common and specific influences. Annu Rev Clin Psychol 2008; 4: 325–348. [PubMed: 18370620]
2. Angoa-Perez M, Kane MJ, Briggs DI, Sykes CE, Shah MM, Francescutti DM, et al. Genetic depletion of brain 5HT reveals a common molecular pathway mediating compulsivity and impulsivity. J Neurochem 2012; 121: 974–984. [PubMed: 22443164]
3. Freeman RD, Fast DK, Burd L, Kerbeshian J, Roberton MM, Sandor P. An international perspective on Tourette syndrome: selected findings from 3500 individuals in 22 countries. Dev Med & Child Neurol 2000; 42: 436–447. [PubMed: 10972415]
4. Burd L, Li Q, Kerbeshian J, Klug MG, Freeman RD. Tourette syndrome and comorbid pervasive developmental disorders. J Child Neurol 2009; 24: 170–175. [PubMed: 19182154]
5. Clarke RA, Lee S, Eapen V. Pathogenetic model for Tourette syndrome delineates overlap with related neurodevelopment disorders including autism. Transl Psychiatry 2012; 2: e158. [PubMed: 22948383]
6. State MW, Greally JM, Cuker A, Bowers PN, Henegariu O, Morgan TM et al. Epigenetic abnormalities associated with a chromosome 18(q21-q22) inversion and a Gilles de la Tourette syndrome phenotype. Proc Nat Acad Sci 2003; 100: 4684–4689. [PubMed: 12682296]
7. State MW. The genetics of Tourette disorder. Curr Opin Genet Dev 2011; 21: 302–309. [PubMed: 21277193]
8. Robbins TW, Vaghi MM, Banca P. Obsessive-Compulsive Disorder: Puzzles and Prospects. Neuron. 2019 Apr 3;102(1):27–47. [PubMed: 30946823]
9. Stein DJ, Costa DLC, Lochner C, Miguel EC, Reddy YCJ, Shavitt RG, van den Heuvel OA, Simpson HB. Obsessive-compulsive disorder. Nat Rev Dis Primers. 2019 Aug 1;5(1):52.
10. Szechtman H, Harvey BH, Woody EZ, Hoffman KL. The Psychopharmacology of Obsessive-Compulsive Disorder: A Preclinical Roadmap. Pharmacol Rev. 2020 Jan;72(1):80–151. [PubMed: 31826934]
11. Hirai H, Pang Z, Bao D, Miyazaki T, Li L, Miura E, et al. Cbln1 is essential for synaptic integrity and plasticity in the cerebellum. Nat Neurosci 2005; 8(11): 1534–1541. [PubMed: 16234806]
12. Uemura T, Lee SJ, Yasumura M, Takeuchi T, Yoshida T, Ra M, Taguchi R, Sakimura K, Mishina M. *Trans*-synaptic interaction of GluRδ2 and Neurexin through Cbln1 mediates synapse formation in the cerebellum. Cell 2010; 141: 1068–1079. [PubMed: 20537373]
13. Matsuda K, Yuzaki M. Cbln family proteins promote synapse formation by regulating distinct neurexin signaling pathways in various brain regions. Euro J Neurosci 2011; 33: 1447–1461.
14. Otsuka S, Konno K, Abe M, Motohashi J, Kohda K, Sakimura K, Watanabe M, Yuzaki M. Roles of Cbln1 in non-motor functions of mice. J of Neurosci 2016; 36(46): 11801–11816. [PubMed: 27852787]
15. Seigneur E, Südhof TC. Genetic ablation of all cerebellins reveals synapse organizer functions in multiple regions throughout the brain. J Neurosci 2018; 38(20): 4774–4790. [PubMed: 29691328]

16. Yuzaki M The C1q complement family of synaptic organizers: not just complementary. Curr Opin Neurobiol. 2017;45: 9–15. [PubMed: 28219683]
17. Südhof TC. Synaptic Neurexin Complexes: A Molecular Code for the Logic of Neural Circuits. Cell. 2017;171(4):745–769. [PubMed: 29100073]
18. Ushkaryov YA, Petrenko AG, Geppert M, and Südhof TC. Neurexins: synaptic cell surface proteins related to the α-latrotoxin receptor and laminin. Science 1992; 257: 50–56. [PubMed: 1621094]
19. Ushkaryov YA, Südhof TC. Neurexin III α: extensive alternative splicing generates membrane-bound and soluble forms. Proc Natl Acad Sci 1993; 90: 6410–6414. [PubMed: 8341647]
20. Ushkaryov YA, Hata Y, Ichtchenko K, Moomaw C, Afendis S, Slaughter CA, Südhof TC. Conserved domain structure of b-neurexins.Unusual cleaved signal sequences in receptor-like neuronal cell-surface proteins. J Biol Chem 1994; 269: 11987–11992. [PubMed: 8163501]
21. Tabuchi K, Südhof TC. Structure and evolution of neurexin genes: insight into the mechanism of alternative splicing. Genomics. 2002;79(6):849–859. [PubMed: 12036300]
22. Südhof TC. Neuroligins and neurexins link synaptic function to cognitive disease. Nature 2008; 455: 903–911. [PubMed: 18923512]
23. Guo SZ, Huang K, Shi YY, Tang W, Zhou J, Feng GY, et al. A case-control association study between the GRID1 gene and schizophrenia in the Chinese Northern Han population. Schizophr Res 2007; 93: 385–390. [PubMed: 17490860]
24. Venken T, Alaerts M, Souery D, Goossens D, Sluijs S, Navon R, et al. (2008) Chromosome 10q harbors a susceptibility locus for bipolar disorder in Ashkenazi Jewish families. Mol Psychiatry 13: 442–450. [PubMed: 17579605]
25. Treutlein J, Muhleisen TW, Frank J, Mattheisen M, Herms S, Ludwig KU, et al. Dissection of phenotype reveals possible association between schizophrenia and Glutamate Receptor Delta 1 (GRID1) gene promoter. Schizophr Res 2009; 111: 123–130. [PubMed: 19346103]
26. Yadav R, Gupta SC, Hillman BG, Bhatt JM, Stairs DJ, Dravid SM. Deletion of glutamate delta-1 receptor in mouse leads to aberrant emotional and social behaviors. PLOS ONE 2012; 7(3): e32969. [PubMed: 22412961]
27. Arnold P, Askland K, Barlassina C, Bellodi L, Bienvenus OJ, Black D, et al. Revealing the complex genetic architecture of obsessive–compulsive disorder using meta-analysis. Mol Psychiatry 2018; 23:1181–1188. [PubMed: 28761083]
28. Gainetdinov RR, Wetsel WC, Jones SR, Levin ED, Jaber M, Caron MG. Role of serotonin in the paradoxical calming effect of psychostimulants on hyperactivity. Science 1999; 283: 397–401. [PubMed: 9888856]
29. Hashimoto H, Shintani N, Tanaka K, Mori W, Hirose M, Matsuda T, et al. Altered psychomotor behaviors in mice lacking pituitary adenylate cyclase-activating polypeptide (PACAP). Proc Natl Acad Sci 2001; 98: 13355–13360. [PubMed: 11687615]
30. Joel D, Doljansky J, Roz N, Rehavi M. Role of the orbital cortex and of the serotonergic system in a rat model of obsessive compulsive disorder. Neuroscience 2005; 130: 25–36. [PubMed: 15561422]
31. Shintani N, Hashimoto H, Tanaka K, Kawagishi N, Kawaguchi C, Hatanaka M, et al. Serotonergic inhibition of intense jumping behvior in mice lacking PACAP (*Adcyap1*$^{-/-}$). Ann NY Acad Sci 2006; 1070: 545–549. [PubMed: 16888223]
32. Li X, Morrow D, Witkin JM. Decreases in nestlet shedding of mice by serotonin uptake inhibitors: Comparison with marble burying. Life Sciences 2006; 78: 1933–1939. [PubMed: 16182315]
33. Amilhon B, Lepicard E, Renoir T, Mongeau R, Popa D, Poirel O, et al. VLGUT3 (vesicular glutamate transporter type 3) contribution to the regulation of serotonergic transmission and anxiety. J Neurosci 2010; 30(6): 2198–2210. [PubMed: 20147547]
34. Greene-Schloesser DM, Ven der Zee EA, Sheppard DK, Catillo MR, Gregg KA, Burrow T., et al. Predictive validity of a non-induced mouse model of compulsive-like behavior. Behav Brain Res 2011; 221: 55–62. [PubMed: 21316394]
35. Sachs BD, Rodriguiz RM, Siesser WB, Kenan A, Royer EL, Jacobsen JPR, et al. The effects of brain serotonin deficiency on behavioral disinhibition and anxiety-like behavior following mild early life stress. Int J Neuropsychopharm 2013; 16: 2081–2094.

36. Wolmarans DW, Brand L, Stein DJ, Harvey BH. Reappraisal of spontaneous stereotypy in the deer mouse as an animal model of obsessive–compulsive disorder (OCD): response to escitalopram treatment and basal serotonin transporter (SERT) density. Behav Brain Res 2013; 256: 545–553. [PubMed: 24013013]
37. Wolmarans DW, Stein DJ, Harvey BH. Excessive nest building is a unique behavioral phenotype in the deer mouse model of obsessive-compulsive disorder. J Pharma 2016; 30(9): 867–874.
38. Seigneur E, Südhof TC. Cerebellins are differentially expressed in selective subsets of neurons throughout the brain. J Comp Neurol 2017; 525: 3286–3311. [PubMed: 28714144]
39. Young KA, Berry ML, Mahaffey CL, Saionz JR, Hawes NL, Chang B, et al. Fierce: a new mouse deletion of Nr2e1; violent behaviour and ocular abnormalities are background-dependent. Behav Brain Res 2002; 132: 145–158. [PubMed: 11997145]
40. Deacon RMJ. Assessing nest building in mice. Nature Protocols 2006; 1(3): 1117–1119. [PubMed: 17406392]
41. Willner P The validity of animal models of depression. Psychopharm 1984; 83: 1–16.
42. Kapur S, Remington G. Serotonin–dopamine interaction and its relevance to schizophrenia. Am J Psychiatry 1996; 153: 466–476. [PubMed: 8599393]
43. Rothman RB, Baumann MH. Balance between dopamine and serotonin release modulates behavioral effects of amphetamine-type drugs. Ann NY Acad Sci 2006; 1074: 245–260. [PubMed: 17105921]
44. Descarries L, Watkins KC, Garcia S, Beaudet A. The serotonin neurons in the nucleus raphe dorsalis of adult rat: a light and electron microscope radioautographic study. J Comp Neurol 1982; 207: 239–254. [PubMed: 7107985]
45. Dorocic IP, Furth D, Xuan Y, Johansson Y, Pozzi L, Silberberg G, et al. A whole-brain atlas of inputs to serotonergic neurons of the dorsal and median raphe nuclei. Neuron 2014; 83: 663–678. [PubMed: 25102561]
46. Zhuang X, Masson J, Gingrich J, Rayport S, Hen R. Targeted gene expression in dopamine and serotonin neurons of the mouse brain. J Neurosci Methods 2005; 143(1):27–32. [PubMed: 15763133]
47. Teissier A, Soiza-Reilly M, Gaspar P. Refining the Role of 5-HT in Postnatal Development of Brain Circuits. Front Cell Neurosci. 2017 May 23;11:139. [PubMed: 28588453]
48. Lee HS, Kim MA, Valentino RJ, Waterhouse BD. Glutamatergic afferent projections to the dorsal raphe nucleus of the rat. Brain Res 2003; 963: 57–71. [PubMed: 12560111]
49. Weissbourd B, Ren J, DeLoach K, Guenthner CJ, Miyamichi K, Luo L. Presynaptic partners of dorsal raphe serotonergic and GABAergic neurons. Neuron 2014; 83: 645–662. [PubMed: 25102560]
50. Geddes SD, Assadzada S, Lemelin D, Sokolovski A, Bergeron R, Haj-Dahmane S, et al. Target-specific modulation of the descending prefrontal cortex inputs to the dorsal raphe nucleus by cannabinoids. Proc Nat Acad Sci 2016; 113(19): 5429–5434. [PubMed: 27114535]
51. Chen A, Hubbert KD, Foroudi PF, Lu VF, Janusonis S. Serotonin 5-HT4 receptors modulate the development of glutamatergic input to the dorsal raphe nucleus. Neurosci Letters 2017; 640: 111–116.
52. Zhou L, Liu M-Z, Li Q, Deng J, Mu D, Sun YG. Organization of functional long-range circuits controlling the activity of sertonergic neurons in the dorsal raphe nucleus. Cell Reports 2017; 18: 3018–3032. [PubMed: 28329692]
53. Herkenham M, Nauta WJ. Afferent connections of the habenular nuclei in the rat. A horseradish peroxidase study, with a note on the fiber-of-passage problem. J Comp Neurol 1977; 173: 123–145. [PubMed: 845280]
54. Herkenham M, Nauta WJ. Efferent connections of the habenular nuclei in the rat. J Comp Neurol 1979; 187: 19–47. [PubMed: 226566]
55. Seigneur E, Polepalli J, Südhof TC. Cbln2 and Cbln4 are expressed in distinct medial habenula-interpeduncular projections and contribute to different behavioral outputs. Proc Nat Acad Sci 2018; 115(43):E10235–E10244. [PubMed: 30287486]

56. Wagner F, Stroh T, Veh R (2014) Correlating habenular subnuclei in rat and mouse by using topographic, morphological, and cytochemical criteria. J Comp Neurol 522:2650–2662. [PubMed: 24478034]
57. Verge D, Daval G, Patey A, Gozlan H, el Mestikawy S, Hamon M. Presynaptic 5-HT autoreceptors on serotonergic cell bodies and/or dendrites but not terminals are of the 5-HT1A subtype. Eur J Pharmacol. 1985;113(3):463–464. [PubMed: 2931289]
58. Fremeau RT, Burman J, Qureshi T, Tran CH, Proctor J, Johnson J, et al. The identification of vesicular glutamate transporter 3 suggests novel modes of signaling by glutamate. Proc Nat Acad Sci 2002; 99(22): 14488–14493. [PubMed: 12388773]
59. Gras C, Herzog E, Bellenchi GC, Bernard V, Ravassard P, Pohl M, et al. A third vesicular glutamate transporter expressed by cholinergic and serotonergic neurons. J Neurosci 2002; 22(13): 5442–5451. [PubMed: 12097496]
60. Soiza-Reilly M, Commons KG. Quantitative analysis of glutamatergic innervation of the mouse dorsal raphe nucleus using array tomography. J Comp Neurol 2011; 519: 3802–3814. [PubMed: 21800318]
61. Gagnon D, Parent M. Distribution of VGLUT3 in highly collateralized axons from the rat dorsal raphe nucleus as revealed by single-neuron reconstructions. PLOS ONE 2014; 9(2): e87709. [PubMed: 24504335]
62. Voisin AN, Mnie-Filali O, Giguere N, Fortin GM, Vigneault E, Mestikawy SE, et al. Axonal segregation and role of the vesicular glutamate transporter VGLUT3 in serotonin neurons. Front Neuroanat 2016; 10: 39. [PubMed: 27147980]
63. Tervo DG, Hwang BY, Viswanathan S, et al. A Designer AAV Variant Permits Efficient Retrograde Access to Projection Neurons. Neuron. 2016;92(2):372–382. [PubMed: 27720486]
64. Ito-Ishida A, Miura E, Emi K, Matsuda K, Iijima T, Kondo T, Kohda K, Watanabe M, Yuzaki M. Cbln1 regulates rapid formation and maintenance of excitatory synapses in mature cerebellar Purkinje cells in vitro and in vivo. J Neurosci 2008; 28(23):5920–5930. [PubMed: 18524896]
65. Takeuchi E, Ito-Ishida A, Yuzaki M, Yanagihara D. Improvement of cerebellar ataxic gait by injecting Cbln1 into the cerebellum of cbln1-null mice. Sci Reports 2018; 8:6184.
66. Yael D, Israelashvili M, Bar-Gad I. Animal models of Tourette syndrome - from proliferation to standardization. Front Neurosci 2016; 10: 132. [PubMed: 27065791]
67. Hirschtritt ME, Darrow SM, Illmann C, Osiecki L, Grados M, Sandor P, et al. Genetic and phenotypic overlap of specific obsessive-compulsive and attention-deficit/hyperactive subtypes with Tourette syndrome. Pscho Med 2018; 48: 279–293.
68. Powell JM, Plummer NW, Scappini EL, Tucker CJ, Jensen P. DEFiNE: A Method for Enhancement and Quantification of Fluorescently Labeled Axons. Front Neuroanat. 2019;12:117. [PubMed: 30687025]

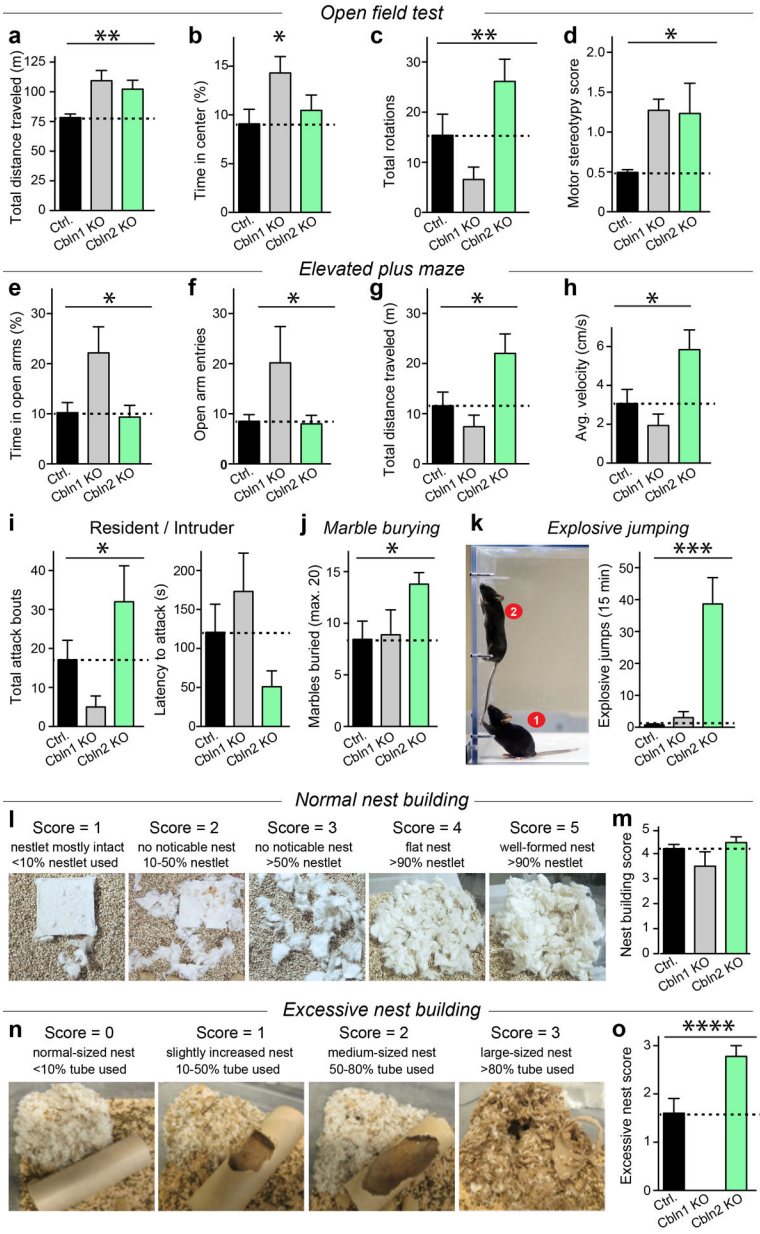

Figure 1: Cbln2 KO mice, but not Cbln1 KO mice, exhibit compulsive jumping and nestbuilding behaviors

(**a–d**) Open field measurements of the spontaneous behaviors of Cbln1 and Cbln2 KO mice on a force-plate actometer (15 min trials; Cbln1 KO, n=8; Cbln2 KO, n=12; controls, n=12). (**a**) Total distance traveled shows that both Cbln1 and Cbln2 mice are hyperactive (**P=0.0049, ANOVA). (**b**) Time spent in the center of the open field suggests that Cbln1 KO mice, but not Cbln2 KO mice, exhibit decreased anxiety (P=0.0981, ANOVA; Cbln1 KO v. Ctrl. adj. *P=0.035, Dunnett's *post hoc*). (**c**) Cbln2 KO mice engage in compulsive circling/running with more rotations than control mice, whereas Cbln1 KO mice make significantly fewer rotations (**P=0.008, ANOVA). (**d**) Measurements of the movement intensity in one place shows that both Cbln1 KO and Cbln2 KO mice display increased motor stereotypy compared to controls (*P=0.032, ANOVA).

(**e**–**h**) Elevated plus maze analyses show that Cbln1 (n=8) but not Cbln2 KO mice (n=9) display decreased anxiety compared to controls (n=10), whereas Cbln2 but not Cbln1 KO mice are hyperactive and engage in compulsive running. (**e**) Cbln1 KO mice spend more time in the open arms (**P*=0.0188, ANOVA) and (**f**) make more entries into the open arms (**P*=0.0424, ANOVA). (**g**) Cbln2 KO mice travel more than twice the distance (**P*=0.0145, ANOVA) on the elevated plus maze with (**h**) twice the speed (**P*=0.0131, ANOVA) than control or Cbln1 KO mice.

(**i**) In the resident/intruder test, Cbln1 KO mice (n=8) exhibit decreased aggression, initiating fewer attacks (left) with a longer latency to attack (right) compared to control mice (n=10; **P*=0.0262, ANOVA). In contrast, Cbln2 KO mice (n=9) show increased aggression, initiating more attacks (left) with a shorter latency to attack (right; *P*=0.0864, ANOVA).

(**j**) Cbln2 KO mice (n=19) but not Cbln1 KO mice (n=9) exhibit compulsive marble burying behavior as compared to control mice (n=16) (**P*=0.0321, ANOVA).

(**k**) Cbln2 KO mice (n=14; 1 month old) display frequent compulsive, novelty-induced explosive jumping behaviors when placed in an open field (force-plate actometer), which is not observed in Cbln1 KO mice (n=8) or control mice (n=10) (****P*=0.0002, ANOVA). Left, composite image depicting a Cbln2 KO mouse before (1) and during (2) an explosive jump; right, summary graph of the number of explosive jumps during a 15 min trial. See Supplementary Video for further information.

(**l** & **m**) Cbln1 KO (n=8), Cbln2 KO (n=9), and control mice (n=10) exhibited similar nest building behaviors during a 24 h period when given a cotton nestlet. Left, example images showing how basic nest building was scored; right, summary graph depicting basic nest building scores.

(**n** & **o**) Cbln2 KO mice (n=9) engage in compulsive excessive nest building, whereas Cbln1 KO mice (n=8) fail to build large nests compared to control mice (n=10) when given a cardboard tube as a nest building material (*****P*<0.0001, ANOVA). Left, example images explaining how excessive nest building was scored; right, summary graph depicting excessive nest building scores.

Data are means ± SEM.

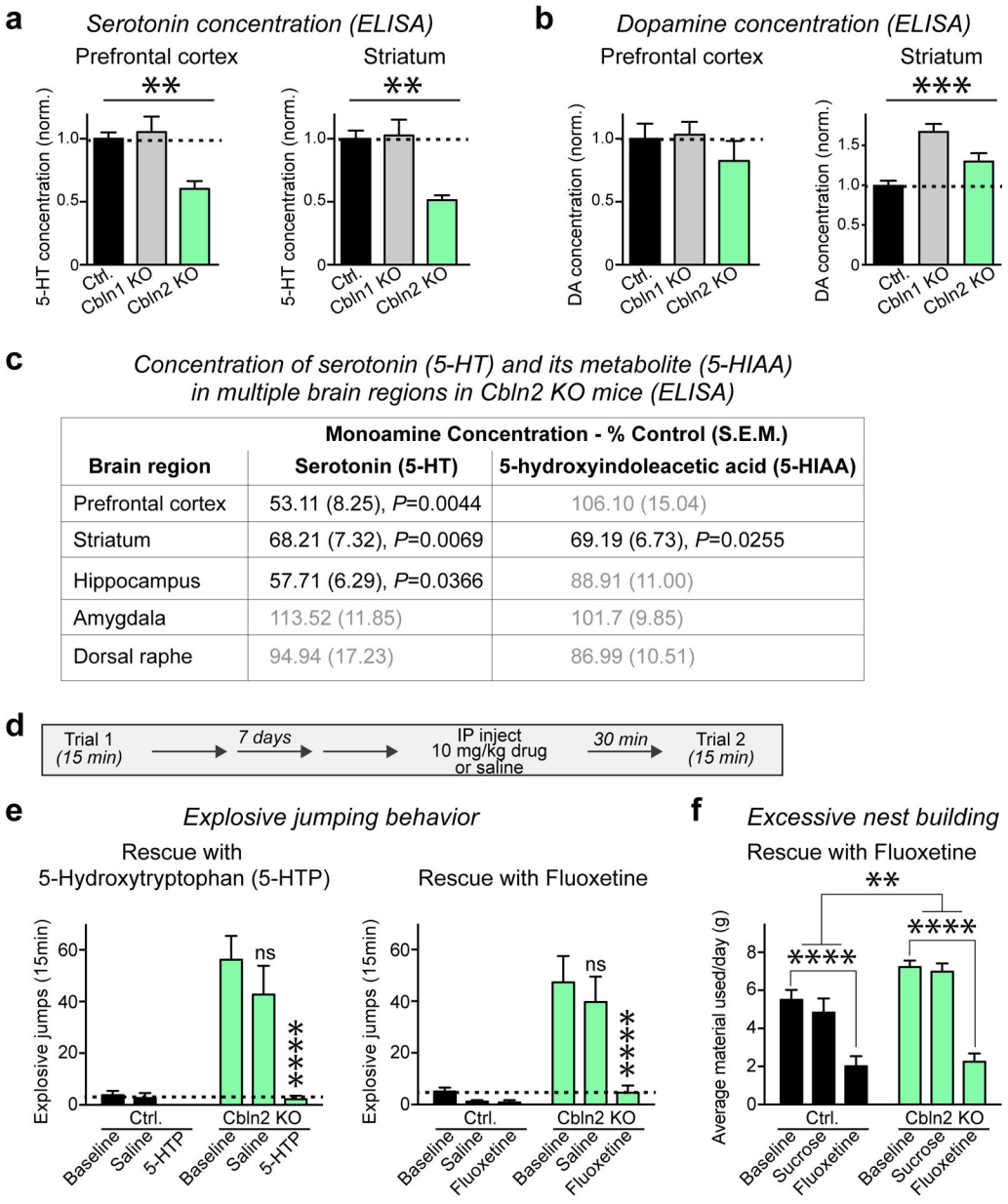

Brain region	Monoamine Concentration - % Control (S.E.M.)	
	Serotonin (5-HT)	5-hydroxyindoleacetic acid (5-HIAA)
Prefrontal cortex	53.11 (8.25), *P*=0.0044	106.10 (15.04)
Striatum	68.21 (7.32), *P*=0.0069	69.19 (6.73), *P*=0.0255
Hippocampus	57.71 (6.29), *P*=0.0366	88.91 (11.00)
Amygdala	113.52 (11.85)	101.7 (9.85)
Dorsal raphe	94.94 (17.23)	86.99 (10.51)

Figure 2: Compulsive behaviors in Cbln2 KO mice are due to serotonergic dysfunction

(**a** & **b**) The serotonin (5-HT) concentrations in the prefrontal cortex (***P*=0.0050, ANOVA) and the striatum (***P*=0.0015, ANOVA) are massively decreased in Cbln2 but not Cbln1 KO mice (**a**), whereas the dopamine concentrations are increased in the striatum (****P*=0.0004, ANOVA) but not prefrontal cortex in Cbln1 and Cbln2 KO mice (**b**). Serotonin and dopamine were measured by ELISA (n=6 samples for each genotype).

(**c**) Concentrations of 5-HT and the 5-HT metabolite 5-HIAA in multiple brain regions. Monoamine concentrations in Cbln2 KO mice are expressed as a percentage control values. Compared to control, 5-HT concentrations in Cbln2 KO mice are decreased in the prefrontal cortex (***P*=0.0044, Student's *t*-Test), striatum (***P*=0.0069, Student's *t*-Test), and hippocampus (**P*=0.0366, Student's *t*-Test), but are unchanged in the amygdala and

dorsal raphe. 5-HIAA concentrations are decreased in the striatum (**P*=0.0255, Student's *t*-Test) but are unchanged in the other brain regions in Cbln2 KO mice.

(**d** & **e**) Explosive jumping behaviors of Cbln2 KO mice are suppressed by treatment with the serotonin precursor 5-hydroxytryptophan (5-HTP) or the serotonin reuptake inhibitor fluoxetine. (***d***) Experimental strategy. 1-month old mice were placed in an open field arena for 15 min to assess baseline explosive jumping behavior. 7 days later, the mice were injected with either saline or 10 mg/kg 5-HTP (or in a separate experiment, saline or 10 mg/kg fluoxetine), allowed to recover for 30 min, and were then placed back into the arena for 15 min to monitor explosive jumps. (***e***) At baseline, Cbln2 KO mice engage in increased jumping behaviors compared to control mice (genotype: *****P*<0.0001, two-way ANOVA). Left, 5-HTP treatment (administered i.p.) dramatically decreases explosive jumping in Cbln2 KO mice (adj. *****P*<0.0001, Tukey's *post hoc*), whereas saline administration has no significant effect (saline n=14; 5-HTP n=20). In contrast, 5-HTP has no effect on jumping behaviors in control mice (saline n=15; 5-HTP n=15). Right, fluoxetine suppresses explosive jumping in Cbln2 KO mice, whereas again saline has no effect (saline n=18; fluoxetine n=16) (adj. *****P*<0.0001, Tukey's *post hoc*). As before, fluoxetine and saline have no effect on jumping behaviors in control mice (saline n= 23; fluoxetine n=18)

(**f**) Excessive nest building is significantly reduced following chronic oral treatment with the serotonin reuptake inhibitor fluoxetine. Mice were given 9 g of cotton nesting material every day for 4 consecutive days and the average daily amount of material incorporated into their nest was measured. Following baseline measurement, mice were given 2% sucrose or 50mg/kg/day fluoxetine in 2% sucrose and nest building was again quantified. Cbln2 KO mice used significantly more nesting material than Ctl mice at baseline and in the 2% sucrose condition (genotype: ***P*=0.0018, two-way ANOVA), and nest building was significantly reduced in both groups following fluoxetine treatment (****adj. *P*<0.0001, Sidak's *post hoc*) (control mice; n=10 sucrose group; n=13 fluoxetine group; Cbln2 KO mice: n=11 sucrose group, n=16 fluoxetine group).

Data shown are mean ±SEM.

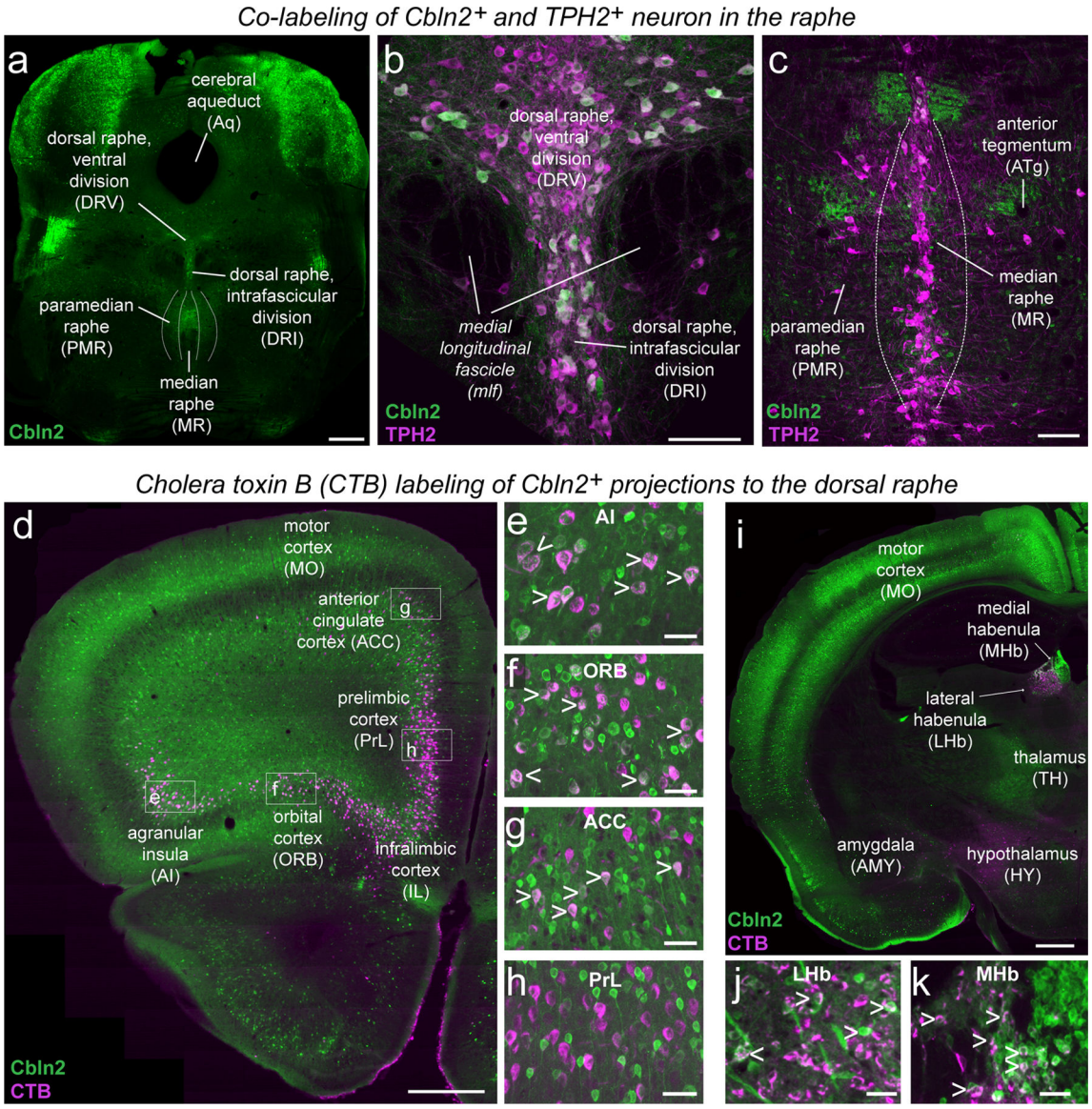

Figure 3: Cbln2 is expressed both in serotonergic neurons in the dorsal raphe (DR) and in non-serotonergic neurons projecting to the DR

(**a**) Coronal section from a Cbln2-mVenus reporter mouse showing Cbln2 expression in the raphe nuclei. Cbln2$^+$ neurons were found primarily in the ventral (DRV) and interfascicular (DRI) subdivisions of the dorsal raphe, with few neurons observed in the dorsal (DRD) and posterodorsal (PDR) subregions. Cbln2$^+$ neurons were also observed in the median raphe (MR) and paramedian raphe (PMR).

(**b**) Double labeling of neurons for Cbln2 (green) and tryptophan hydroxylase 2 (TPH2; magenta) in the DRV and DRI. Cbln2 expression was visualized using an antibody to GFP.

(**c**) Same as in (b) but showing the median raphe (MR) and the paramedian raphe (PMR).

(**d**) Coronal section of the mPFC from a Cbln2-mVenus reporter mouse following injection of the retrograde tracer cholera toxin B (CTB) into the DR.

(**e**–**h**) Higher magnification images of the boxed areas in panel d illustrating that Cbln2$^+$ neurons that are CTB$^+$ and thus project to the DR were observed in the agranular insular

cortex (AI; **e**), orbital frontal cortex (ORB; **f**), and to a lesser degree, the anterior cingulate cortex (ACC; **g**). However, although both $Cbln2^+$ and CTB^+ neurons were observed in the prelimbic (PrL) and infralimbic (IL) cortical areas, there was almost no overlap between the two populations (arrowheads = double-positive neurons).

(**i**) Same as d, but at a more caudal level to illustrate the presence of CTB^+ and $Cbln2^+$ neurons in the lateral (LHb) and medial (MHb) habenula.

(**j**) A large number of CTB^+ neurons that project to the DR were observed in the LHb and most of these neurons were co-labeled for Cbln2.

(**k**) Only a small number of CTB^+ neurons were observed in the MHb and nearly all of these neurons were co-labeled for Cbln2.

Scale bars = 500 μm (a, d, i), and 100 μm (b–c, e–h, j–k). Abbreviations: AMY, amygdala; ATg, anterior tegmental nucleus; Aq, cerebral aqueduct; HY, hypothalamus; mlf, medial longitudinal fascicle; MO, motor cortex; TH, thalamus.

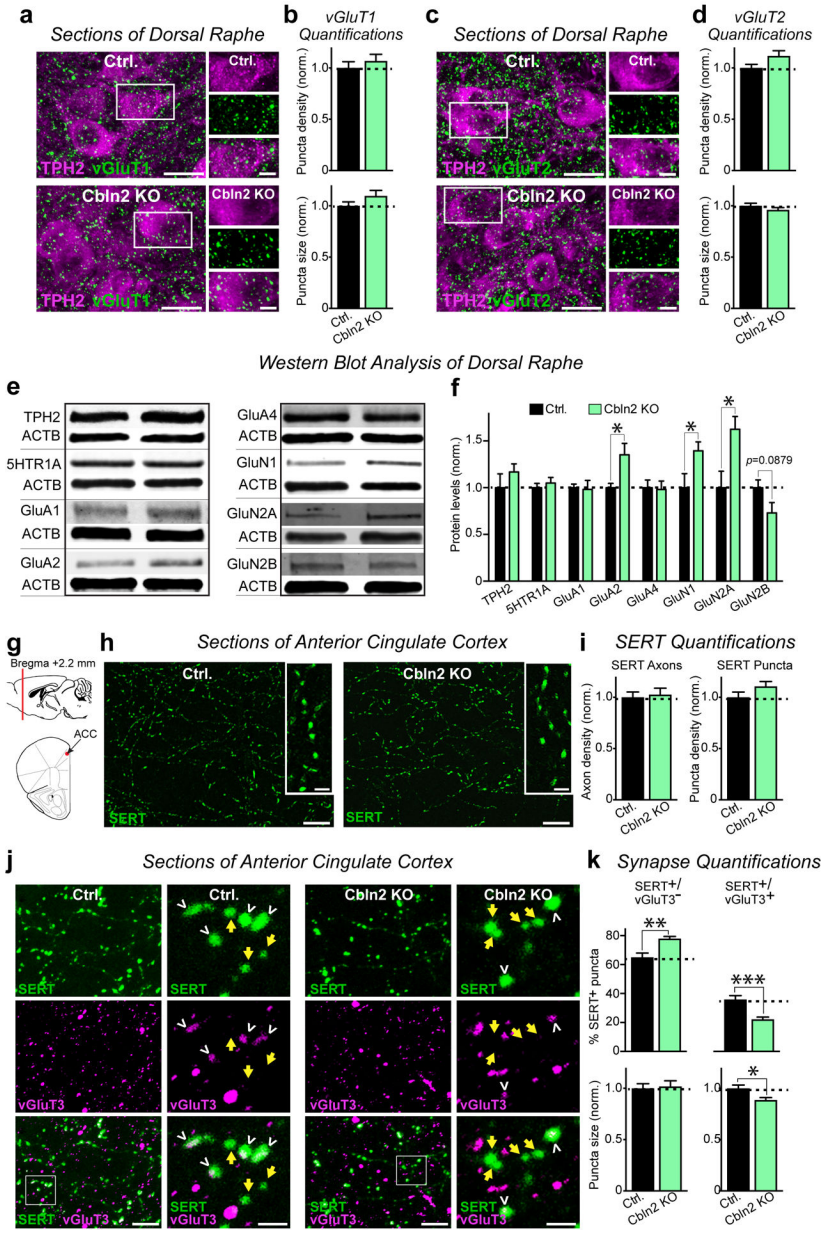

Figure 4: The constitutive Cbln2 KO increases glutamate receptor levels in the dorsal raphe and decreases the vGluT3 content of serotonergic nerve terminals in the anterior cingulate cortex without changing synapse densities

(**a & c**) Representative immunofluorescence images of sections from the dorsal raphe (DR) of control *(top)* and Cbln2 KO (*bottom*) mice aged P30–35. Sections were co-labeled with TPH2 (magenta) to identify serotonergic neurons and vGluT1 (*a*) or vGluT2 (*c*) to mark excitatory puncta (green). Cutouts show single-channel images of the boxed region. Scale bar = 20 μm.

(b & d) Summary graphs showing that deletion of Cbln2 has no effect on the density *(top)* or size *(bottom)* of vGluT1^{+} (*b*) or vGluT2^{+} (*d*) puncta on TPH2^{+} neurons in the DR. All data are means ± S.E.M.; synaptic puncta density was normalized to the area

of TPH2-labeled tissue and to the levels observed in the controls. Statistical analysis was performed by Student's *t*-Test (n = 3 sections/mouse, 3 mice/genotype).

(**e & f**) The Cbln2 KO induces an increase in the levels of the AMPAR subunit GluA2 (**P*=0.0101, Student's *t*-test) and of the NMDAR subunits GluN1 (**P*=0.0494, Student's *t*-test) and GluN2A (**P*=0.0464, Student's *t*-test) in the dorsal raphe (*e*, representative immunoblots; *f*, summary graphs). Proteins from littermate control and Cbln2 KO mice aged P30–35 were analyzed by quantitative immunoblotting. Data are means ± S.E.M. (n=6 mice/group); data were normalized first to the levels of β-actin as an internal loading control, and then to the controls.

(**g**) Schematic showing the location of the anterior cingulate cortex (ACC) sections shown and quantified in h–k.

(**h & i**) Loss of Cbln2 has no effect on the density of axons or puncta expressing serotonin reuptake transporter (SERT) in the ACC. (**h**) Representative fluorescence images showing SERT antibody labeling in the ACC of ~1 month old control (*left*) and Cbln2 KO (*right*) mice. Inserts show a high magnification example of $SERT^+$ puncta. Scale bars = 25 μm. (**i**) Summary graphs showing the density of $SERT^+$ axons (*left*) and puncta (*right*) in the ACC of control and Cbln2 KO mice. Data shown are means ± S.E.M. Axon density was quantified using the DEFiNE plugin for ImageJ. Axon and puncta density were first normalized to the area of the region of interest and then to the levels observed in the controls. Statistical analysis was performed by Student's *t*-test (n = 3 sections/mouse, 3 mice/genotype).

(**j & k**) Loss of Cbln2 increases the relative density of synaptic puncta expressing serotonin reuptake transporter (SERT) but not vGluT3, but decreases the density and size of presynaptic puncta expressing both SERT and vGluT3 on axons projecting from the DR to the ACC. (**j**) Representative images showing antibody labeling of SERT (green) and vGluT3 (magenta) in sections of ACC taken from ~1 month old control (*left*) and Cbln2 KO mice (*right*). Scale bars = 25 um. (**k**) Summary graphs showing an increase in the percentage of $SERT^+$ puncta that lack vGluT3 ($SERT^+/vGluT3^-$ puncta; ***P*=0.0015, Student's *t*-Test), and a decrease in the percentage of $SERT^+$ puncta that contain vGluT3 ($SERT^+/vGluT3^+$ puncta; ****P*=0.0005, Student's *t*-Test) in the ACC of Cbln2 KO mice compared to control (*top*). Additionally, there was a small but significant decrease in the size of the $SERT^+/vGluT3^+$ puncta in the Cbln2 KO mice (**P*=0.0117, Student's *t*-test) but not in the $SERT^+/vGluT3^-$ puncta (*bottom*). Data shown are means ± SEM and were normalized to the levels observed in the controls (n = 3 sections/mouse, 3 mice/genotype).

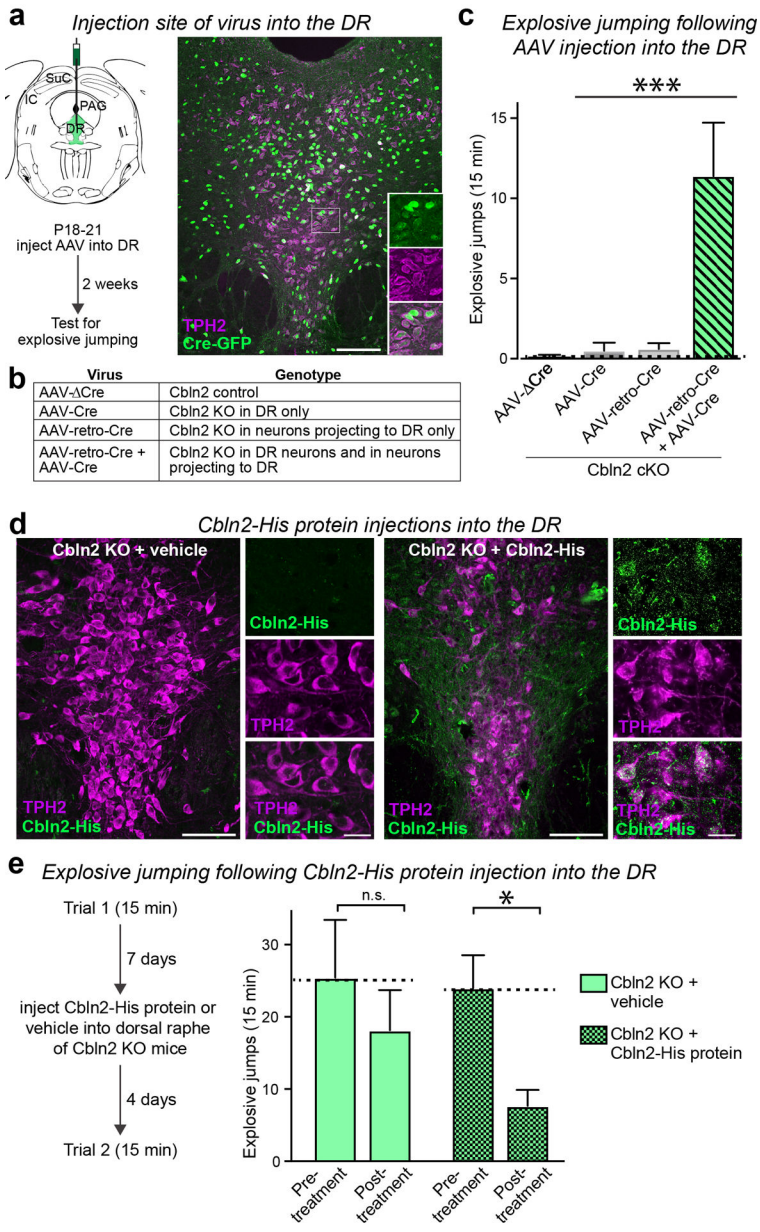

Figure 5: Cbln2 deletions induce explosive jumping of mice when Cbln2 is ablated both from DR neurons and from neurons projecting to the DR, while explosive jumping in Cbln2 KO mice can be rescued by stereotaxic injection of recombinant Cbln2 protein into the DR

(**a**) Schematic showing the site of stereotaxic virus injections into the DR of Cbln2 cKO mice (*left*), and representative image showing expression of GFP (green) following injection of AAV-retro-Cre + AAV-Syn-Cre-GFP into the DR of Cbln2 cKO mice (*right*). Serotonergic neurons are co-labeled with TPH2 (magenta). Scale bar = 100 μm.

(**b**) Table showing the combination of viruses used and the resulting genotype.

(**c**) Combined deletion of Cbln2 from neurons projecting to the DR and from neurons in the DR (AAV-retro-Cre + AAV-Cre; n=23) produces explosive jumping behavior. Explosive jumping was rarely observed in control mice (AAV-ΔCre; n=18), following deletion of Cbln2 from only the DR (AAV-Cre; n=14), or following deletion of Cbln2 only from

neurons projecting to DR (AAV-retro-Cre; n=18). ***P=0.0002, ANOVA. Data are means ± SEM.

(**d**) Representative images showing the distribution of injected Cbln2-His protein (or vehicle), labeled with anti-His antibody (green), in the DR 2 days post-injection. Serotonergic neurons are labeled with TPH2 (magenta). Higher magnification images show the puncate pattern of Cbln2-His labeling on the dendrites and cell bodies of $TPH2^+$ neurons (*right*), which is absent in the vehicle treated sections (*left*). Scale bars = 100 um, and 20 um in higher magnification images.

(**e**) (*left*) Schematic depicting the experimental protocol. (*right*) Explosive jumping was significantly decreased in Cbln2 KO mice following injection of recombinant Cbln2-His protein into the DR compared to baseline (adj.*P=0.0127, Sidak's *post hoc*) and vehicle injected mice (treatment: P=0.0291, two-way ANOVA). Vehicle treated mice n=7, Cbln2 treated mice n=9. Data shown are mean ± SEM.